

Probabilistic Modeling of the Aeroelastic Life Cycle for Risk Evaluation of Composite Structures

Andrey V. Styuart¹, Luciano Demasi², Eli Livne* and Kuen Y. Lin*

Department of Aeronautics and Astronautics, University of Washington, Seattle, WA, 98195-2400

Virtual aeroelastic tests using Monte Carlo simulations can be used to quantify the aeroelastic reliability of damage-tolerant composite aircraft structures, enabling aircraft manufacturers, operators, and flight certification authorities to establish design, maintenance and service guidelines that reduce lifecycle cost. A probabilistic / reliability methodology and computer simulation capability for composite airframes is presented in this paper and used to study a simple isotropic delta wind tunnel model and a realistic vertical tail / rudder system of a transport airplane.

Nomenclature

σ_{VF}	=	standard deviation of flutter speed
σ_p	=	standard deviation of parameter
C_v	=	coefficient of variation
F_{VA}	=	cumulative probability distribution function (CDF) of maximum random airspeed per life
f_{VF}	=	probability density function (PDF) of random flutter speed.
N_f	=	number of flights per life.
P_f	=	probability of failure
V_F	=	flutter speed
V_D	=	max diving speed
V_A, V	=	airspeed
R_{cor}	=	radius of correlation
W	=	total cross-section width of finite element
W_D	=	maximum cross-section of damage size normal to the direction of the applied load
$\kappa_{T(U)}$	=	original tensile stiffness of the composite
$\kappa_{T(D)}$	=	tensile stiffness of the damage region
$\kappa_{C(U)}$	=	original compressive stiffness of the composite
$\kappa_{C(D)}$	=	compressive stiffness of the damage region, which is negligible for hole.

I. Introduction

THIS paper is devoted to the extension of the available **RE**liability-based **L**ifecycle **A**nalysis of **C**omposite **S**tructures method and corresponding software RELACS¹⁻⁴ to the aeroelastic reliability problem. The method and software have been developed at the University of Washington with support from the FAA and the Boeing Company to provide a tool for evaluating the damage-tolerance of composite structures based on strict reliability criteria rather than general phenomenological considerations. This probabilistic approach encompasses a large number of variables to provide a realistic description of the problem, including material properties, environmental variables, damage statistics, maintenance practices, etc. The method had been tested in cases of structural strength problems. In the work reported herein it was applied to aeroelastic risk analysis.

In general, the **RE**liability-based **L**ifecycle **A**nalysis of **C**omposite **S**tructures software accepts any failure definition including aeroelastic failure. In the case of flutter, failure may be defined as the event $V_A > V_F$ when the

¹ Acting Assistant Professor, Department of Aeronautics and Astronautics, Box 352400.

² Research Associate, Department of Aeronautics and Astronautics, Box 352400

* Professor, Department of Aeronautics and Astronautics.

airspeed V_A exceeds the flutter speed V_F of a structure in a flow field. Both V_A and V_F are uncertain quantities and may be characterized by appropriate probability measures. Such characterizations are the most crucial for reliability assessment. There is considerable statistical data gathered to allow characterization of the probability density function (PDF) of the airspeed V_A . (e.g. ref. 5-6). Very little statistical data, however, is available to allow evaluation of the PDF of the flutter speed V_F . This limited data is mostly based on the results of modal tests of full-scale structures (measuring the scatter in structural dynamic properties of different airframes of the same vehicle at different times during its service life) and can not be used for V_F without additional substantiation. The only alternative to actual tests of a large enough sample of vehicles is the utilization of virtual tests using a mathematical aeroelastic model with simulation of appropriate elementary uncertainties, such as ones of structural stiffness, mass, etc. In this way the statistical characterization of flutter speed and flutter frequency, as well as free vibration characteristics, may be achieved. The study of the correlation between structural dynamic and resulting flutter quantities may give an answer to the interesting question of whether the scatter of natural structural frequencies can be used for flutter speed (V_F) statistical characterization.

The present study focuses on uncertainty in structural characteristics of airframes, and so the essential part of the RELACS input data preparation is the statistical characterization of uncertain structure. There were quite a number of attempts to obtain statistical characteristics of flutter and aeroelastic limit-cycle-oscillations (LCO) such as those presented in Ref. 7-16.

Different computational methodologies have been employed to quantify the uncertain response of aeroelastic structures with parametric uncertainty. In finite element modeling of aeroelastic phenomena, uncertainties are usually introduced into the stiffness parameters and the stiffness is usually represented by a random field. The problem has been tackled through Monte Carlo simulation or stochastic finite element methods (e.g. perturbation method or Neumann expansion method). Due to the large number of samples required, which require a high computational effort, the Monte Carlo simulation has been usually used mainly to verify other approaches. The perturbation and Neumann expansion methods had been shown to lead to acceptable results for small random variation in the material properties. It was found that these methods are comparable in accuracy, but that the most efficient solution procedure is the perturbation finite element method, which requires a single simulation. The perturbation stochastic finite element method has been adopted by several researchers using the Karhunen-Loeve expansion to discretize the random fields due to structure mechanical properties. However, perturbation methods require the system uncertainty to be small enough to guarantee convergence and accurate results.

Structural and material uncertainties have a direct impact, of course, on the flutter characteristics of aeroelastic structures, and published references to date report statistical studies of the flutter of panels and shells¹⁰⁻¹⁶. Uncertainties in mass density, air density, and in-plane loads were also considered. References 13-14 consider uncertainties in the modulus of elasticity and also boundary conditions for a nonlinear panel in supersonic flow and the probabilistic response distributions were obtained using Monte Carlo simulation. In references 15-16 a first-order perturbation method was employed to solve for the probability of flutter given uncertainty in the structural mass and stiffness operators. Again, the focus of most work to-date in this area has been on the assessment of accuracy of predictions based on approximate statistical methods relative to Monte Carlo simulation.

In the work presented here Monte Carlo simulations were used to carry out virtual tests in an effort to gain insight into statistical aeroelastic scatter of realistic aeroelastic systems, and the issue of accuracy of approximate statistical methods was of minor interest. The reasons: with current finite element / linear flutter prediction simulation capabilities one complete flutter run takes only a half minute for simplified realistic structures such as a 762-element plate-wing flutter model and 67 seconds for a very representative 3169-element vertical tail / rudder model on dual core PC processor. There is also no big confidence increment by simulating millions of flutter samples compared to thousands if the underlying structural element property statistical distributions are based on only a relatively small number of coupon tests (10 or so) per property, as limitation of schedule and budget would usually allow.

Instead, the present work pays most attention to the following: The shape of the PDF of the flutter speed V_F ; The probabilistic sensitivity of V_F to various random properties variations; The effect of various properties correlation on the PDF of V_F , especially the effect of spatial correlation on the PDF of V_F and the effect of elementary property scatter on the average V_F (scale effect); The relationship between the variance of elementary properties and V_F variance; The effect of skin damages on the PDF of V_F . and the effect of skin damages on the resulting reliability.

II. The University of Washington's Virtual Testing Tools for Composite Aircraft

The University of Washington's Virtual Test Laboratory (UWVTL) tool, developed at the University of Washington Aeronautics and Astronautics department, is aimed at large-scale, structural/aeroelastic systems. It allows virtual proof-testing of designs prior to or in parallel with their structure development. The major applications driving development of the UWVTT are advanced composite structures of civil aircraft.

To better understand virtual aeroelastic tests an aircraft design process can be imagined in which it is required to prove that the structure is free from flutter. Traditionally, flutter analysis, structural modal tests, and flight tests using applicable methods would be used. The real structure tested, however, is not exactly the structure analyzed because the properties used (thicknesses, material properties, dimensions, etc.) are slightly different from those used in the analysis. In addition, the method of analysis has some finite accuracy. As a result test results would probably differ from analytical prediction. From a statistical point of view, the difference doesn't necessarily mean that the mathematical model has to be modified or the structure reinforced. If the difference falls within the possible scatter of test results, the math model and test structure can be acceptable but with a need to understand and explain why they are different.

The usual problem is that the measured scatter is unknown. Actual testing additional structures just to measure the scatter is expensive and impractical. It is much easier and practical to use mathematical simulations – virtual testing – to study the effects of parameter variations on overall behavior of interest.

An important aspect of virtual testing for airframes is the ease in which the effects of changes in structural properties and material parameters can be examined. As the mathematical model is usually of the Finite Element (FE) type, changing input parameters can be time consuming due to the complexity of the FE package and models used. Computational time per case, which adds up rapidly when models' complexity and detail rise, is another factor to consider. The UWVTL is designed to accelerate analysis and input data variation and to be truly interactive (with the addition of a graphical interface and user friendly interaction with the model input parameters). The two main UWVTT parts are the VATM module for virtual aeroelastic tests and the RELACS module for time-dependent virtual tests.

III. VATM: Quantification of structural response uncertainty.

VATM is a virtual aeroelastic test module designed primarily for characterization of the variability of typical aeroelastic response quantities such as structural eigenfrequencies or flutter speed. Reliability tools included in RELACS require statistical input data which are not routinely obtained in current design and substantiation processes. Some data may be obtained through extensive and expensive testing programs. The accuracy of probabilistic analysis relies heavily on the accuracy of input. When experimental data is not available from full-scale physical testing, results obtained by Finite Element Analysis (FEA) and other deterministic methods with random inputs may be used instead as virtual experiments.

The current VATM procedure consists of six steps.

1) Construction of the structural finite element analysis (FEA) structural model. This step is made outside of the VATM software and may involve any FEA preprocessor. In the current study MD/MSC PARTAN has been used for structural model preparation and post-processing of eigenmodes. The NASTRAN input file for modal analysis is prepared based on nominal thicknesses and material properties. In general, each finite element of the model should have its own property card and material card.

2) Aeroelastic model construction. Here unsteady aerodynamic mesh, reduced frequencies, and atmospheric and flight condition inputs are added. The NASTRAN flutter analysis code capability is used for a solver. Flutter and aerodynamic entries have been added to the NASTRAN input file created previously (step 1) for Normal Modes/Eigenvalue NASTRAN input.

3) To obtain the randomly varied test structures, the property and materials cards of the NASTRAN input file are changed by the appropriate Microsoft VBA-based module. The way the randomized cards are generated is described at the end of this section.

4) The VATM runs the solver using the randomized input file.

5) After the solver (NASTRAN) completes its run, the appropriate output file is analyzed by VATM module to obtain normal modes/eigenfrequencies and flutter velocity and frequency. The output data along with some input data are accumulated and stored in a database.

6) After a certain number of steps 3-5 runs, VATM conducts the statistical analysis of the data obtained.

In general, automation of aeroelastic response predictions for cases involving large model variations is not trivial. In the linear case, when flutter speeds are sought, robust root tracking and interpolation algorithms are required in order to reliably follow the evolution of root locus branches as functions of dynamic pressure and overcome challenges posed by mode switching. In the nonlinear aeroelastic case (limit cycle oscillations, for example), measures of dynamic response must be identified and used in order to reflect effects of variations in the structure on resulting response time histories. The problem of analysis automation and results extraction is common to statistical studies of the effects of system's variability, parametric trend studies, and design optimization studies.

Some probabilistic aeroelastic studies to date involve simple aeroelastic models with the spatially distributed uncertainties considered in a form of Markov field. The covariance kernel of the random field is often assumed in the form:

$$C(x, x_1) = \sigma_p^2 e^{-\frac{|x-x_1|}{R_{cor}}} \quad (1)$$

Where σ_p^2 is a field variance and R_{cor} is a radius of correlation.

In the present study the correlation of properties and material parameters reflects expected characteristics of structural subcomponents that are manufactured separately and then assembled. The properties of individual finite elements belonging to skin panels, spars, stringers, and frames are considered correlated within each panel, spar, etc., respectively. Properties of structural subcomponents manufactured separately are assumed independent.

In certain conditions, if a standard deviation σ grows and becomes comparable with the average value of stiffness, aeroelastic instability may occur, which had been observed by some researchers. At the same time it is known from the test of coupons cut from the same panel that variation of property of composites within one panel is rather small compared to the variation of the same property between panels¹⁹. This guides a quite specific method of stochastic FEA simulation of realistic aerospace structures: Markov field simulation for panels with random average values simulated independently for each panel or other structural subcomponent.

In order to provide the input data for RELACS, the present work considers the influence of stiffness and mass uncertainties on the flutter behavior of two test cases: (1) a simple trapezoidal aeroelastic wing of constant thickness made of isotropic material (Plexiglas), and (2) an aeroelastic vertical tail with a rudder made of carbon reinforced fiber composites CFRP. The first case (Refs. 18, 19) corresponds to well-known modeling and wind tunnel experiments at Duke University, but is modified compared to the Duke model. The second case is a representative vertical tail / rudder system similar to that of a passenger airplane. Both structures are made of CFRP material. As realistic structures are assembled from several independently manufactured subcomponents, direct Monte-Carlo simulation of average panel properties and Markov field simulation have been used.

IV. RELACS – Time-Dependent Virtual Testing.

RELACS is created for virtual life testing. In this method, described in Refs. 1-3, the structural damage size life histories (as well as material degradation and structural changes due to environmental effects) are simulated using randomized input parameters. These are converted into the histories of residual structural property subject to environmental exposures, repairs, and other factors. The residual property may be strength, stiffness, flutter speed, vibration level, etc. depending on the considered failure mode (see Figure 1). Random loading and flight conditions are also generated in the form of mechanical load / temperature / airspeed histories and compared to the structural property statistics (stress, deformation, flutter speed, etc.) to find if failure can occur. That is, statistics of changes of structural behavior over time (with resultant change, in, say, flutter speed) are compared to statistics of loading and flight conditions (say, actual flight speeds and dynamic pressures) over time to evaluate the probability that failure (actual flight speed exceeds flutter speed) will occur. In another example, the statistics of residual strength are compared to actual loading histories to find the probability that actual loading will lead to stresses above buckling or yield limits). The number of failures per total number of simulated life histories yields the probability of failure (POF).

The University of Washington's Reliability Lifecycle Analysis of Composite Structures (RELACS, Refs. 1-3) method and associated software can be used to determine any controllable parameters in the structural system required to achieve a prescribed level of reliability. Design parameters that affect structural reliability can be actual sizes (thicknesses) of structural elements, topology and load paths in the structure, material type, joint type and strength, etc. But important design parameters that affect the reliability of the system are also inspection/repair methods, their time and place.

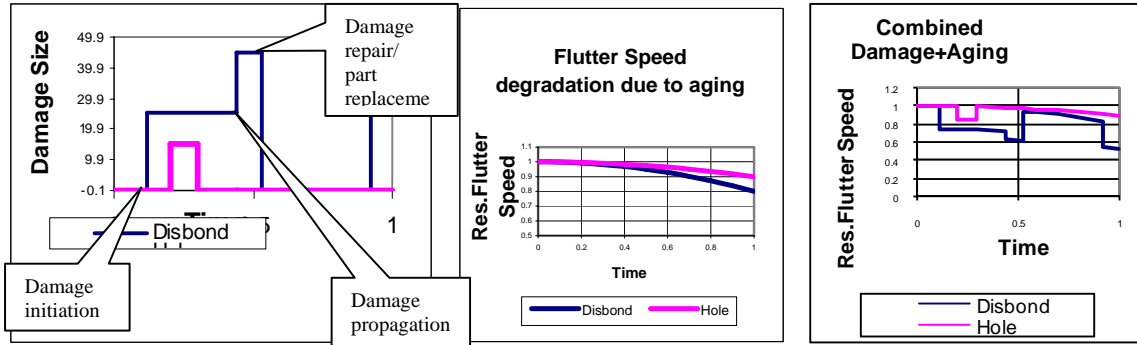


Figure 1: Simulated Histories of residual flutter speed variation with time, as affected by damage, aging, and repair

Now, inspection/repair/replacement planning is one of the most important design tools for meeting damage tolerance requirements and managing damage-induced risk, whether purely structural or aeroelastic. In reality, maintenance is affected by many parameters such as availability of inspection methods, availability of repair tools, inspectors/repairer skill levels, repair decisions, costs, etc. The University of Washington's method can take into account such parameters and estimate the risk (expected losses) associated with any particular maintenance plan. So far several practical and important real-case example problems have been solved, in particular: Reliability-based damage-tolerance of a composite aileron of commercial aircraft¹; Probabilistic disbond propagation for typical bonded skin-stringer panel of an aft fuselage of a commercial aircraft; Probability of failure (POF) due to flutter for a realistic damage-tolerant composite flaperon (Ref. 9) on a supersonic fighter; Optimum maintenance planning for vertical tail of commercial aircraft (Ref. 2).

V. Extension of RELACS to the Aeroelasticity Problem

The RELACS model and software have been extended to the aeroelastic failure due to structural changes. The key elements of such extension of the method and tools are:

A. A Probabilistic model for Extreme Operational Environments

Currently, failure is recorded in the event that a one-dimensional environmental / loading factor (dynamic stress due to gust, airspeed, etc) exceeds one-dimensional critical structural property (strength, flutter speed). Such failure modes as high amplitude LCO or gust response (and fatigue) can be characterized not only by the random combination of two factors such as airspeed and initial excitation, but also by the preceding history of dynamic excitation. As LCO and thermal effects are not considered in the current study, only extreme equivalent airspeed is used here. The cumulative density function (CDF) F_{Va} for maximum flown airspeed per life has been obtained from an exceedance curve by an asymptotic formula (Ref. 6):

$$F_{Va}(V/V_D) = \exp\{-\exp[F(V/V_D)] \cdot N_f\} \quad (2)$$

where $F(V/V_D)$ is the probability of speed exceedance per one flight, and N_f is a number of flights per life. In Ref. 6, conservative parameters of F_{Va} were obtained and this CDF is cast in a form.

$$F_{Va}(V/V_D) = F_{Va}(z) = \exp\left[-\exp\left(-\frac{z-1}{0.0063}\right)\right] \quad (3)$$

Where $z = V/V_D$.

B. Complex failure mode uncertainty quantification

The statistical data and assumptions used to characterize structural variations in elements of the airframe are discussed in subsequent sections which cover the delta wing and the vertical tail / rudder tests cases. Monte-Carlo simulation of failure conditions for complex systems with random parameters can capture different uncertainty propagation (from determining parameters to final behavior) related to different failure modes. They can also capture another important feature: critical failure modes may change (or switch) for the same operational conditions

due to system parameters variance. One interesting case is a critical flutter mechanism change due to structural variation. As it will be shown later, this may happen even within reasonable range of parameters variations. If the focus is critical flutter speed, then a switch in the set of modes that leads to critical flutter may not be captured by approximate methods based on sensitivity analysis.

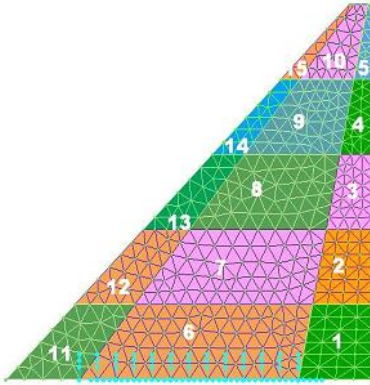


Figure 2: Simple Wing Panels and Mesh

VI. Uncertain Aeroelastic Finite Element Model of Simple Wing

The finite element mesh for the first wing under consideration is shown in Figure 2. This simple wing is a plate, and it was artificially divided into 15 panels to allow for representation of panel-to-panel variability. All structural panels have been simulated using SHELL finite elements with randomized thickness and three random material properties for an isotropic material: Young's modulus, Poisson ratio, and material density. Average panel properties and materials were simulated independently, while those of elements belonging to each panel were simulated using a Markov random field. The correlation matrix is calculated according to Eq.(1) with R_{cor} as measured between the element centroids. One of the well-known methods to obtain the correlated random vector of normally-distributed element's properties, is correlation matrix factorization (See: http://www.columbia.edu/~mh2078/MCS04/MCS_framework_FEegs.pdf). Then the lower triangular matrix $\{c_{ij}\}$ is multiplied by a vector of independently generated random values $\{\xi_i\}$ with zero mean and unit

variance (Eq.4). To obtain correlated element properties $\{x_i\}$, the resultant vector of correlated values $\{\zeta_i\}$ with zero means and unit variances is multiplied by property standard deviation σ and the vector of average values $\{a_i\}$ is added.

$$\begin{matrix} \text{Factorization} & \text{Lower matrix} \\ \left\{ \begin{matrix} r_{11} & \cdots & r_{1n} \\ \vdots & \ddots & \vdots \\ r_{n1} & \cdots & r_{nn} \end{matrix} \right\} \Rightarrow \left\{ \begin{matrix} c_{11} & 0 & 0 \\ \vdots & \ddots & 0 \\ c_{n1} & \cdots & c_{nn} \end{matrix} \right\} \left\{ \begin{matrix} \xi_1 \\ \vdots \\ \xi_n \end{matrix} \right\} = \left\{ \begin{matrix} \zeta_1 \\ \vdots \\ \zeta_n \end{matrix} \right\} \Rightarrow \left\{ \begin{matrix} x_1 \\ \vdots \\ x_n \end{matrix} \right\} = \sigma \left\{ \begin{matrix} \zeta_1 \\ \vdots \\ \zeta_n \end{matrix} \right\} + \left\{ \begin{matrix} a_1 \\ \vdots \\ a_n \end{matrix} \right\} \end{matrix} \quad (4)$$

The flutter problem has been solved using NASTRAN¹⁹ SOL145 PK method with doublet-lattice aerodynamics, 402 aerodynamic panels at Mach=0, without structural damping. Uncertainties of aerodynamic parameters have not been considered in the work discussed here.

C. Results of virtual tests

The following results were obtained using the data on coefficient of variation and correlation radius for elements with PSHELL properties given in Table 1.

Table 1

Property	Panel-to-panel C.O.V.	Element-to-element C.O.V.	Radius of Correlation, in
Thickness t	0.03	0.01	10
E	0.05	0.02	100
<i>Poisson ratio</i>	0.05	0.02	100
<i>Density</i>	0.05	0.02	100

Figure 3 shows the empirical CDF of Flutter velocity obtained by Monte-Carlo for 1000 runs of the NASTRAN model with four random parameters per element (three material properties and thickness). The CDF is very close to the Gauss distribution when we assumed the Weibull PDF for elementary properties. According to the theory of probability this is characteristic for the sum of many random variables.

Experiments with other popular PDFs resulted in similar Gauss-type curves. It is worth noticing that the coefficient of variation of V_F is less than those of elementary properties.

Figure 4 shows the probabilistic sensitivities of V_F to the average panel material Young's modulus (E) random variation. The selected measure of sensitivity is the regression slope V_F/E normalized by the standard deviation of V_F and standard deviation of modulus.

$$S = SLOPE(V_F, E) \sigma_E / \sigma_{V_F}$$

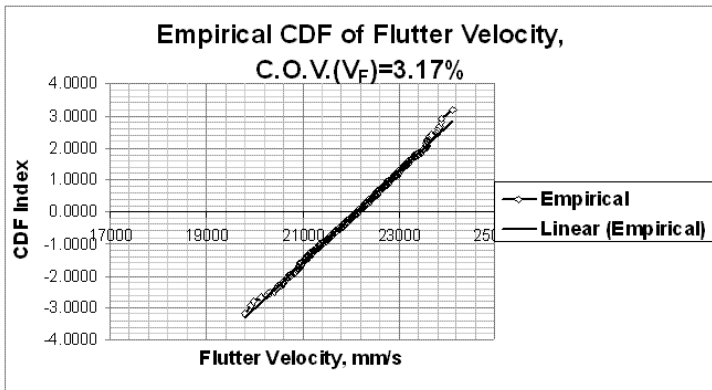


Figure 3: CDF of Flutter Speed in Normal CDF scale.

Figure 5 shows the probabilistic sensitivities of V_F to random variation of panel material density ρ . The measure of sensitivity is similar to the above mentioned: the regression slope V_F/ρ normalized by the standard deviation of V_F and standard deviation of the density.

Note the larger effect of variation of stiffness along the “elastic axis” of the wing, which determines bending and effective torsion stiffness. Mass (density) variation seem to lead to larger effects when present in elements along the leading and trailing edges as well as the wing tip with the potential, overall, of larger effects on natural frequencies of mass away from the elastic axis (torsion) and the wing tip (bending).

Figure 6 shows the probabilistic sensitivities of V_F to random variation average panel thickness t . The measure of sensitivity is similar to the above mentioned: the regression slope V_F/t normalized by standard deviation of V_F and standard deviation of density. The sensitivity of flutter speed to stiffness along the wing’s “elastic axis” (even though this is a plate and not a high aspect ratio beam wing) is evident.

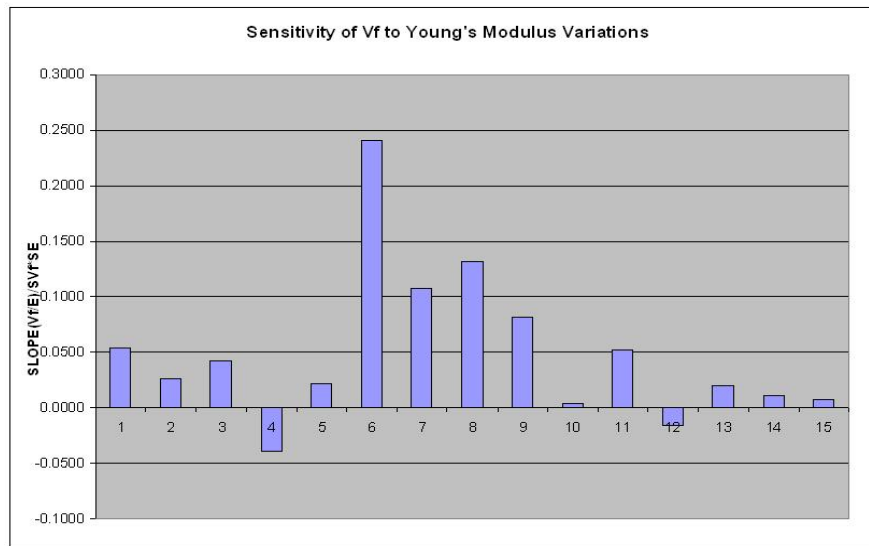


Figure 4: V_F Sensitivity to Average Panel Modulus Variations

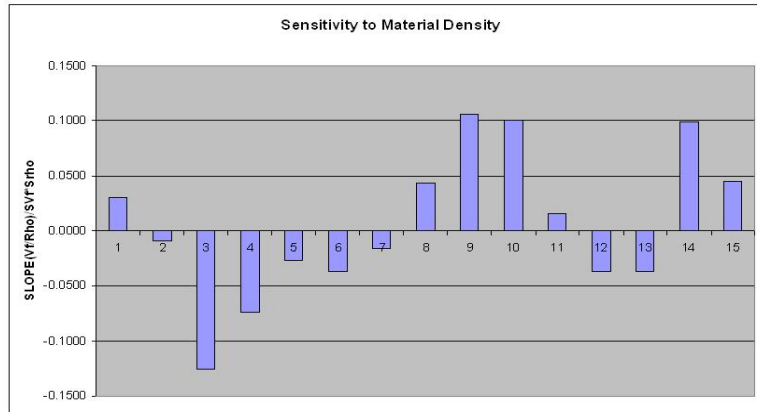


Figure 5: V_F Sensitivity to Average Panel Density Variations

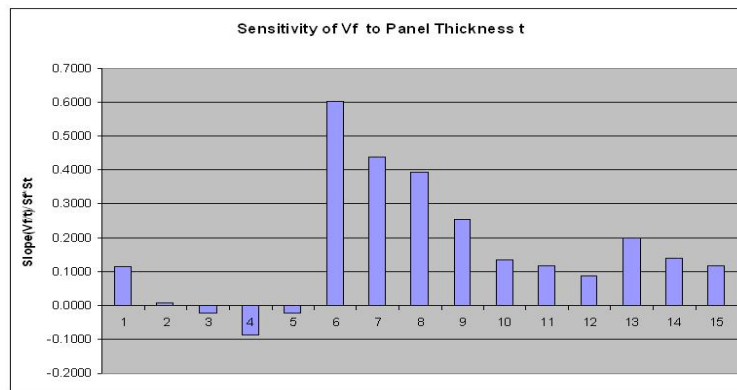


Figure 6: V_F Sensitivity to Average Panel Thickness Variations

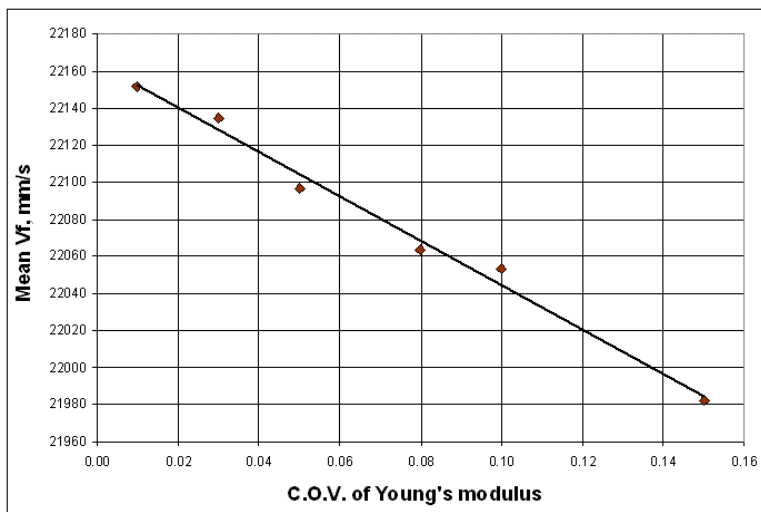


Figure 7. Mean Flutter Velocity vs. C.O.V. of E

Figure 7 shows another important result: The average flutter velocity depends on the variance of Young's modulus. Fortunately the average Flutter velocity decrease with increase of modulus scatter by less than 1 percent in realistic range of modulus scatter. This effect is similar to the effect typical to a "weakest link model", when the response of complex system is defined by it weakest link. The bigger is the scatter of properties the lower is the property value of the weakest link. Practically it means that the real expected flutter speed of the wing with substantial scatter of properties will be lower that that obtained using nominal values of properties. The simple model under consideration has only

few “weakest elements” located near the wing root on Panel 6. That is why this effect is so small. It should be expected that more complicated and more optimized models will exhibit more considerable effect.

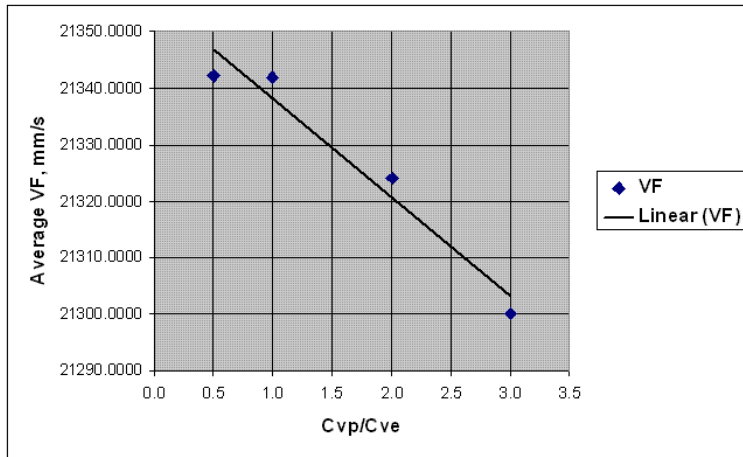


Figure 8: Effect of Cvp/Cve ratio on V_F

As this effect is present, it is also interesting to see how it is changed depending on the relationship between the panel-to-panel property variation and element-to element variation.

Figure 8 shows how the average V_F changes depending on the ratio between C.O.V. of panel-to-panel mean E and C.O.V. of element-to element E. Evidently, the panel-to-panel scatter plays the most important role in the statistical effect on flutter velocity in this case.

Additional parametric studies were conducted in the course of this work. The effect of correlation between neighboring finite elements

properties is shown in Figure 9.

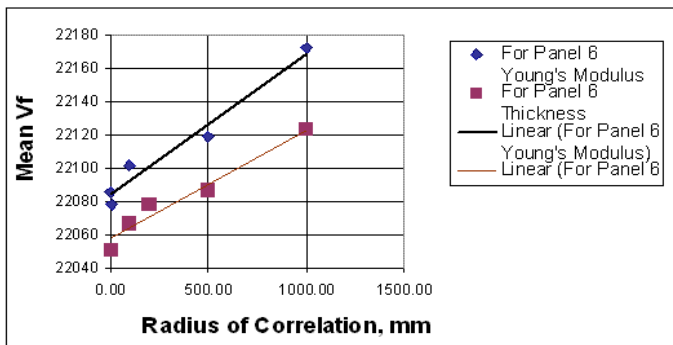


Figure 9: Average Flutter Velocity vs. Radius of Correlation

Figure 9 shows that there is slight dependency of the average flutter speed V_F on the Markov field radius of correlation for thickness and Young’s modulus. As has been mentioned above, this effect may be stronger in the case of an optimized structure with elevated property scatter.

It also has been assumed that a correlation between some material properties may exist. Such properties as modulus and density may, for example, be correlated due to porosity of polymer material. It may be especially visible for compression failure modes when fiber micro-buckling to the pores takes place.

The effect of this correlation has been also evaluated. Figure 10 shows the average V_F for various correlation

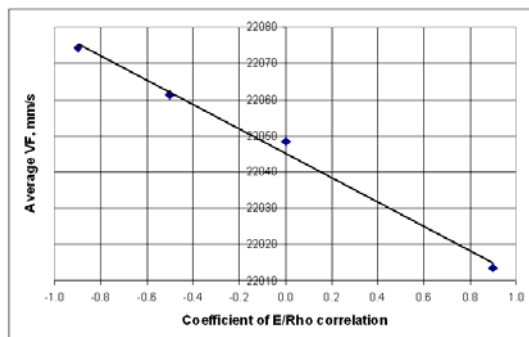


Figure 10: Average Flutter Velocity vs. E/ρ Correlation



Figure 11: Average Flutter Velocity vs. Expected Damage

coefficients E/ρ . As it may be expected the negative increment of E and positive increment of density lead to lower the flutter velocity, as it is shown in Figure 10.

D. Effect of damage

To illustrate the effect of damage on flutter velocity PDF, damage has been simulated as appropriate loss of element stiffness. A number of damaged element and the damage size have been simulated according to the data taken from Ref 6. The damage intensity has been scaled as if the wing under consideration were a real-size aircraft wing. The locations of damaged elements have been chosen randomly with uniform distribution over the wing area. Figure 11 shows the average residual V_F depending on the expected damage size per life. The C.O.V. of V_F is slowly increasing with the damage size.

VII. The Uncertain Aeroelastic Vertical Tail / Rudder System

A realistic NASTRAN model of a composite vertical tail / rudder system of a passenger airplane (but not representing any actual flying vehicle) is presented in Fig. 12. The nodes at the root end of spars were fixed.

The model random input is characterized by the data shown in Table 1. The model was modified with VATM to allow every structural and mass element to have its own property and material card. The elements belonging to structural panels which are manufactured separately were united into groups to represent panel-to-panel variability.

Table 2

Number of grid points	1268
Number of CBAR elements	309
Number of CBUSH elements	45
Number of CONM2 elements	28
Number of CQUAD4 elements	1409
Number of CROD elements	1056
Number of CSHEAR elements	91
Number of CTRIA3 elements	187
Number of RBE2 elements	16
Number of RBE3 elements	28

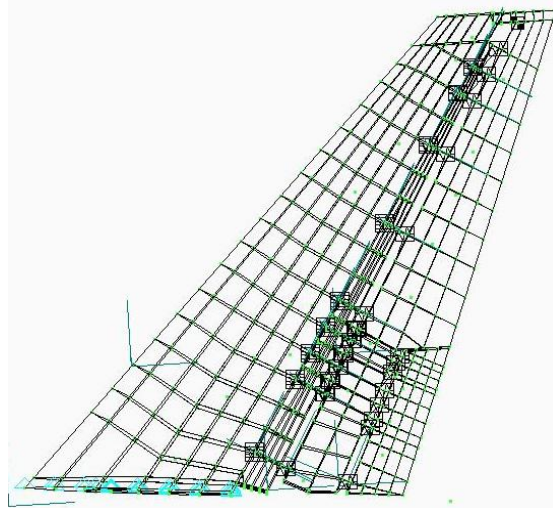


Figure 12: Representative Vertical Tail FEA Model

Attention was paid to adequate simulation of the composite skin panels where impact damages were expected. Those structural panels were simulated using NASTRAN SHELL finite elements with randomized thickness and three random material properties: G_{11} , G_{12} , and G_{22} . Since the model arrived from industry with lumped masses representing mass distribution for dynamics purposes, the material density was simulated as included in those lump masses. The correlation between thickness and structural mass was simulated due to the lack of appropriate information for this particular model. Average panel geometric and materials properties were simulated independently, while those of individual finite elements belonging to each panel were simulated using the Markov random field in the same way as for simple delta wing model.

E. Aerodynamic model

Figure 13 shows the aerodynamic model used for the vertical tail rudder system. The unsteady aerodynamics is based on the Doublet Lattice Method (Ref. 20 and 21). The aerodynamic reference surface on the plane $x-z$ is divided into 5 trapezoidal macropanels (see Figure 14). Each macropanel is subdivided into strips of trapezoidal panels. Surface splining for information transmission between structural and aerodynamic points is taken care of by the software (MD NASTRAN). It should be noted that in this model the trapezoidal surfaces 1, 2 and 3 (see Figure 13) have the same number of aerodynamic elements in the wing span direction. Similarly, surfaces 4 and 5 have the same number of aerodynamic elements in the wing span direction. The root of the structural model of the vertical

tail was not exactly parallel to the axis of the incoming flow. Therefore, the aerodynamic reference surface was slightly adjusted to make the root exactly directed in the x direction.

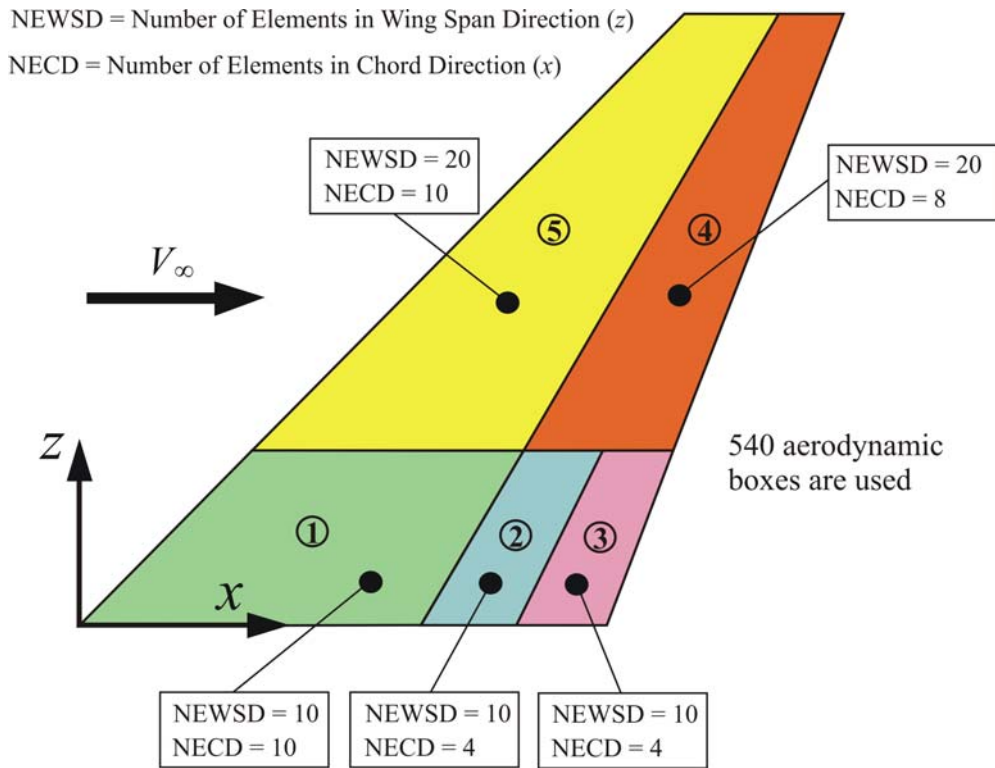


Figure 13: Vertical Tail: Aerodynamic Model (Doublet Lattice Method)

F. Free vibration virtual test results

Figure 14 and figure 15 show, for illustration, the free vibration mode shapes of the nominal structure with eigenfrequencies close to flutter frequency of about 13 Hz. Actual natural modes contributing to the flutter mechanism can vary, depending on variations in the structure and possible switching of flutter mechanisms, depending on the magnitude and combination of structural perturbations.

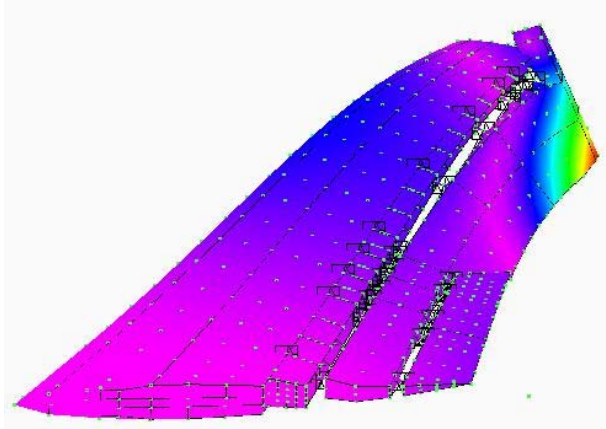


Figure 14: Free Vibration Mode Shape of the nominal structure, Frequency = 16.34Hz

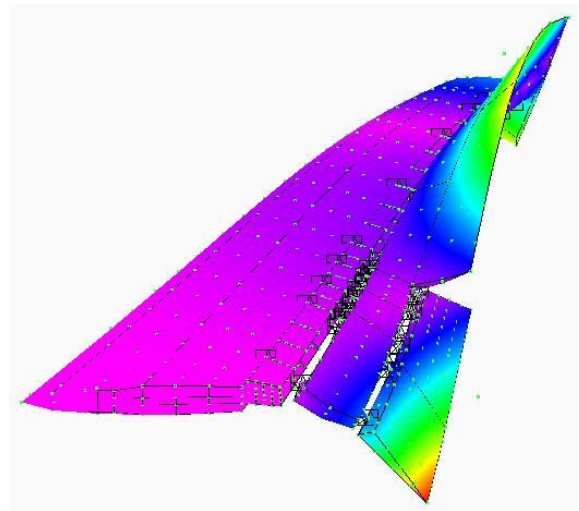


Figure 15: Free Vibration Mode Shape of the nominal structure; Frequency = 18.24Hz

G. Virtual Flutter Test Results

The following results were obtained using the data on variances and correlations for elements with PSHELL properties given in Table 3.

Table 3

Property	Panel-to-panel C.O.V.	Element-to-element C.O.V.	Radius of Correlation, in
Thickness t	0.03	0.01	10
G_{11}	0.05	0.02	100
G_{22}	0.05	0.02	100
G_{12}	0.05	0.02	100

The typical C.O.V. values of Table 2 parameters were taken from MIL-HDBK-17. Theoretically the radius of correlation could be also evaluated from the data of the MIL-HDBK-17, if the appropriate supporting information like panel size, coupon size were present there. The C.O.V. of thickness and Young's modulus for PBAR and PROD properties were assumed equal to 0.02. The same value has been used for CONM2 mass elements.

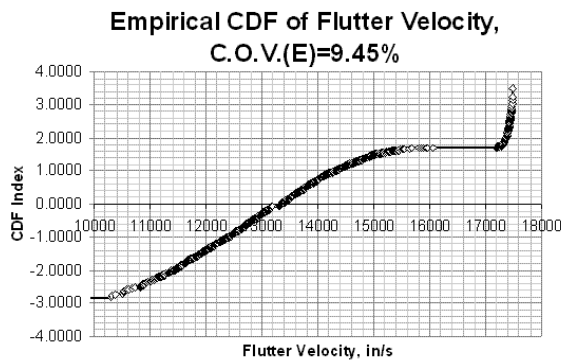


Figure 16: CDF for Vertical Tail Flutter Velocity

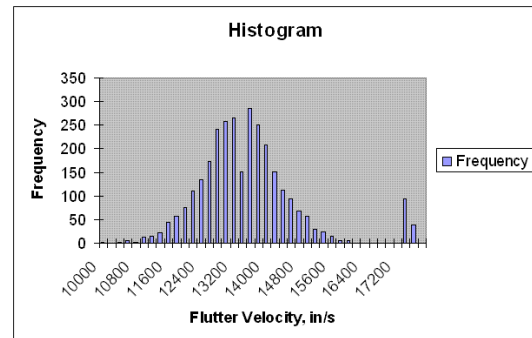


Figure 17: Flutter Velocity Histogram

The most interesting results of the virtual tests are shown in Figure 16 and Figure 17. Figure 16 shows the empirical CDF of flutter velocity. It is obvious that the corresponding PDF is bimodal. This fact is reflected in Figure 17, where the corresponding histogram is shown. Practically this means that some aircraft in a fleet simulated using the assumptions listed above, may have the flutter frequency and flutter mechanisms rather different from main population. It is also evident that the variance of the second flutter mechanism is much smaller than the first one. This may be an evidence of the different uncertainty propagation for different failure modes mentioned earlier. In this particular case, the second mode of PDF is on the left tail of distribution which contributes to the greater safety. But there may be situations when this mode may appear on the left tail. It is also obvious that some popular fast reliability methods like SORM, FORM (Ref. 24, 25) may generally not be applicable to the probabilistic study of flutter and similar aeroelastic phenomena.

Another observation is that the variance of V_F is noticeably greater than variances for input parameters shown in Table 2. This is rather different from what was observed in the simple delta wing model.

H. Damaged Structure Tests

Figure 18 shows the empirical CDF of V_F obtained with VATM under the condition that a randomly selected element belonging to the tail torsion box skin has big damage of the size of about 150 mm.

Only stiffness reduction due to damage was considered and estimated (by using analysis of the element itself) as the difference of average relative displacements of opposite nodes per given loading depending on damage size. The

damage was assumed at a center of the element. The locations of damaged elements have been chosen randomly with uniform distribution over the tail box skin area.

As in Ref. 6, the residual stiffness has been determined using expressions based upon a rule-of-mixtures for constant thickness panel:

$$\begin{aligned}\kappa_T &= \left(\frac{W - W_D}{W}\right) \kappa_{T(U)} + \left(\frac{W_D}{W}\right) \kappa_{T(D)}; \\ \kappa_C &= \left(\frac{W - W_D}{W}\right) \kappa_{C(U)} + \left(\frac{W_D}{W}\right) \kappa_{C(D)}\end{aligned}\quad (5)$$

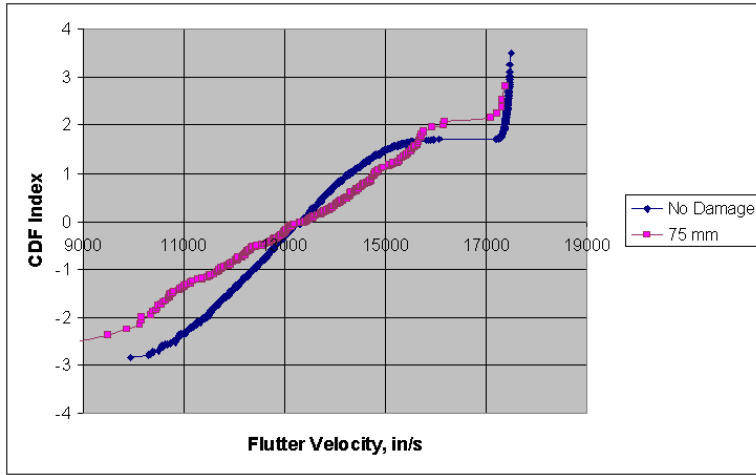


Figure 18: Empirical CDF of V_F for damaged and undamaged structure

element centroid.

The V_F CDF for the undamaged structure is shown in Figure 18 for comparison. It is interesting to notice that the average values are almost the same, but the C.O.V of the damaged structure is much greater. This behavior is rather different from one obtained for simple model where the average decreases with the damage size, but C.O.V. remains nearly constant. Both behaviors will inevitably lead to lower reliability.

VIII. Time-dependent study with RELACS

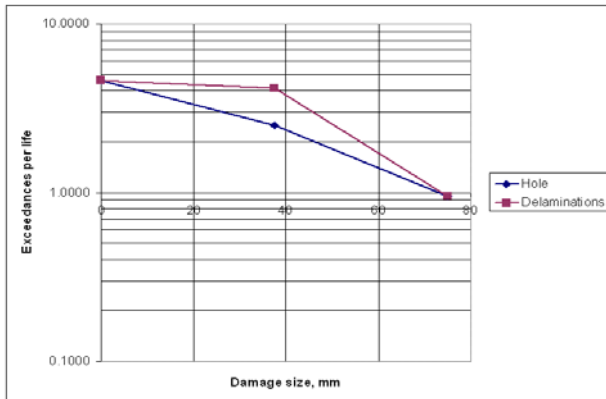


Figure 19: Damage Exceedance Curve

where:

W is the total cross-section width of an element, $W=250 - 450\text{mm}$

W_D is the maximum cross-section of damage size normal to the direction of the applied load,

$\kappa_{T(U)}$ is the original tensile stiffness of the composite,

$\kappa_{T(D)}$ is the tensile stiffness of the damage region, which is negligible for hole,

$\kappa_{C(U)}$ is the original compressive stiffness of the composite,

$\kappa_{C(D)}$ is the compressive stiffness of the damage region, which is negligible for hole.

The cross-section width of an element has been defined for each randomly selected element in the direction coinciding with an aircraft longitudinal axis at the position of

The input data for RELACS were taken from Ref. 6. Panel weight change due to repair was not presently considered due to the lumped mass nature of both structural and nonstructural mass in the model. The V_F CDF for undamaged structure and damaged structure were taken by polynomial approximation of curves shown in Figure 18 and other curves obtained with VATM for different damage sizes.

The following input data was used:

- Number of Design Cases = 1; Subsonic flight
- Number of Damage Types = 2; Hole and Delamination
- Number of Inspection Types = 2; Visual and Instrumental

- The CDF of maximum airspeed per life is expressed by equation (3).
- The probability of damage detection model described in Ref. 6 was used.
- The exceedance data of damage occurrence is taken from Ref. 23 and recalculated for 60000 flight hours and torsion box skin area. The corresponding plot is shown in Figure 19. To introduce even more conservatism, the damage sizes in the calculations were twice larger than those of Figure 19. This might include the damages inflicted by uncontained turbine blades and similar cases.

Figure 20 shows the Probability of Failure accounting for damage depending on the safety margins used for design. The POF without damages as a function of the safety margin used for design is also shown for comparison.

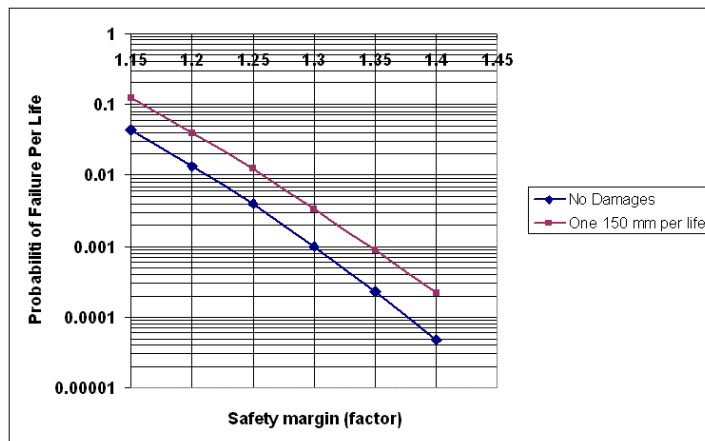


Figure 20: POF vs. Safety Margin (Factor)

simulation capabilities developed for this work and described above can be used to identify such cases and to study them and the consequences for design and maintenance.

It should be mentioned that the representative vertical tail / rudder system here has about 57% safety margin above V_D by design and it is highly safe.

The probabilistic analysis shows that in order to ensure the same POF as in no-damage case, the safety margin with nominal stiffness should be at least 5% greater than that without damage considerations. This conclusion, it should be emphasized, is not general and is case dependent. Situations may occur, for some airframe designs, where damage or combination of damages that lead to partial local loss of stiffness or increased mass may lead to flutter failures. The

Conclusions

Virtual aeroelastic tests using Monte Carlo simulations can be used to quantify the reliability of damage-tolerant composite aircraft structures, enabling aircraft manufacturers, operators, and flight certification authorities to establish design, maintenance and service guidelines that reduce lifecycle cost. A probabilistic / reliability methodology and computer simulation capability for composite airframes was presented in this paper and used to study a simple isotropic delta wing wind tunnel model as well as a realistic vertical tail / rudder configuration of a passenger airplane.

The possible switching of flutter mechanisms for some structural properties variations can lead to multimodal response probability density. In such cases some popular fast reliability methods like SORM, FORM are generally not applicable to the probabilistic study of flutter and similar aeroelastic phenomena. Uncertain aeroelastic models can exhibit the properties of “weakest-link” configurations, with scale effects that should be taken into account when uncertainties of structural properties are expected to be larger than usual. These uncertainties include spatial correlations of properties such as thickness, modulus, density, etc. and correlations between material properties like stiffness and density, and various components of anisotropic material stiffness matrix. Composite structures are currently the most exposed to this phenomenon.

Acknowledgments

This work was supported under the Federal Aviation Administration Research Grant, "Combined Global/Local Variability and Uncertainty in Integrated Aeroservoelasticity of Composite Aircraft". Peter Shyprykevich, Curtis Davies, and Dr. Larry Ilcewicz were grant monitors. The authors wish to thank the FAA and the FAA Center of Excellence at the University of Washington (AMTAS) for sponsoring the current research project. Thanks to the Boeing Commercial Airplane Group for help and support, especially the construction of the vertical tail / rudder system NASTRAN model used here.

References

- ¹ K. Lin and A. Styuart, "Probabilistic Approach to Damage Tolerance Design of Aircraft Composite Structures", *Journal of Aircraft*, Vol. 44 No. 4, 2007, pp. 1309-1317.
- ² A. Styuart and K. Lin "Maintenance Planning for Aircraft Damage Tolerant Composite Structures Based on Risk Assessment", AIAA-2007-1979, 48th AIAA/ASME/ASCE/AHS/ASC Structures, Structural Dynamics, and Materials Conference, Honolulu, Hawaii, Apr. 23-26, 2007
- ³ K Y. Lin and A. V. Styuart, "A Reliability Method for Assessing Damage Severity in Composite Structures", 38th ITC - Dallas, Texas - Nov 6-9, 2006
- ⁴ C.H. Cheung, A.V. Styuart, K.Y.Lin, "Reliability of Composite Structures with Damage Growth Consideration," ASC 22nd Annual Technical Conference, Seattle, WA, September 17-20, 2007
- ⁵ Taylor, J., "Manual on aircraft loads", Oxford, New York, Published for and on behalf of Advisory Group for Aeronautical Research and Development, North Atlantic Treaty Organization by Pergamon Press, 1965
- ⁶ A. Styuart, M. Mor, E. Livne, and K. Lin, "Aeroelastic Failure Risk Assessment in Damage Tolerant Composite Airframe Structures" AIAA-2007-1981 48th AIAA/ASME/ASCE/AHS/ASC Structures, Structural Dynamics, and Materials Conference, Honolulu, Hawaii, Apr. 23-26, 2007
- ⁷ Pettit, C. L., "Uncertainty Quantification in Aeroelasticity: Recent Results and Research Challenges" *Journal of Aircraft*, Vol. 41, No.5 2004, pp 1217-1229.
- ⁸ Pettit, C. L., "Uncertainty Quantification in Aeroelasticity: Recent Results and Research Challenges," *Journal of Aircraft*, Vol. 41, No. 5, 2004, pp. 1217-1229.
- ⁹ Pettit, C. L., and Beran, P. S., "Effects of Parametric Uncertainty on Airfoil Limit Cycle Oscillations" *Journal of Aircraft*, Vol. 40, No.5 2004, pp 1217-1229.
- ¹⁰ Liaw, D. G. and Yang, H. T. Y., "Reliability of Uncertain Laminated Shells Due to Buckling and Supersonic Flutter," *AIAA Journal*, Vol. 29, No. 10, 1991, pp. 1698-1708.
- ¹¹ Liaw, D. G. and Yang, H. T. Y., "Reliability of Initially Compressed Uncertain Laminated Plates in Supersonic Flow," *AIAA Journal*, Vol. 29, No. 6, 1991, pp. 952-960.
- ¹² Kuttenukeuler, J. and Ringertz, U., "Aeroelastic Tailoring Considering Uncertainties in Material Properties," *Structural Optimization*, Vol. 15, Nos. 3/4, 1998, pp. 157-162.
- ¹³ Lindsley, N. J., Beran, P. S. and Pettit, C.L., "Effects of Uncertainty on the Aerothermoelastic Flutter Boundary of a Nonlinear Plate," AIAA Paper 2002-5136, 2002.
- ¹⁴ Lindsley, N. J., Beran, P. S. and Pettit, C. L., "Effects of Uncertainty on Nonlinear Plate Aeroelastic Response," AIAA Paper 2002-1271, 2002
- ¹⁵ Poirion, F., "Impact of Random Uncertainty on Aircraft Aeroelastic Stability," Proceedings of the 3rdrd International Conference on Stochastic Structural Dynamics, San Juan, PR, 1995.
- ¹⁶ Poirion, F., "On Some Stochastic Methods Applied to Aeroservoelasticity," *Aerospace Science and Technology*, Vol. 4, No. 3, 2000, pp. 201-214.
- ¹⁷ Attar P.J., Dowell E.H., White J.R., "Modeling the LCO of a Delta Wing Using a High Fidelity Structural Model", 45th AIAA/ASME/ASCE/AHS/ASC Structures, Structural Dynamics & Materials Conference, Palm Springs, California, Apr. 19-22, 2004.
- ¹⁸ Attar P.J., Dowell E.H., White J.R., "Modeling Delta Wing Limit-Cycle Oscillations Using a High-Fidelity Structural Model", *Journal of Aircraft* Vol. 42, No. 5, September-October 2005
- ¹⁹ Schaeffer, H.G., MSC.NASTRAN Primer for Linear Analysis, second edition, MSC Software, Santa Ana, CA, 2001.
- ²⁰ Rodden W. P., Taylor P. F., McIntosh Jr S.C., "Further Refinement of the Subsonic Doublet-Lattice Method", *Journal of Aircraft*, Vol. 35 No. 5, 1998
- ²¹ Albano E., Rodden W. P. "A Doublet-Lattice Method for Calculating Lift Distributions on Oscillating Surfaces in Subsonic Flows", *AIAA Journal*, Vol. 7, No. 2, 1969
- ²² Livne, E., "Integrated Aeroservoelastic Optimization: Status and Progress", *Journal of Aircraft*, Vol. 36, No. 1, January-February 1999, pp. 122-145.
- ²³ Ushakov A., Stewart A., Mishulin I., and Pankov A. "Probabilistic Design of Damage Tolerant Composite Aircraft Structures", U.S. Dept. of Transportation, Federal Aviation Administration, Report DOT/FAA/AR-01/55, Washington DC, January 2002
- ²⁴ NESSUS Theoretical Manual. Southwest Research Institute. Version 7.0 October 2001
- ²⁵ Long M. W., and Narciso J. D., "Probabilistic Design Methodology For Composite Aircraft" U.S. Dept. of Transportation, Federal Aviation Administration, Report DOT/FAA/AR-99/2, Washington DC, June 1999